

Reliability assessment of existing concrete bridges with geometrical NDT results – case studies

Dr.-Ing. Stefan Kütttenbaum *
Dipl.-Ing. Christian Kainz **
Univ.-Prof. Dr.-Ing. Thomas Braml **

* BAM – Federal Institute for Materials Research and Testing, Div. 8.2, Berlin, Germany, stefan.kuettenbaum@bam.de

** University of the Bundeswehr Munich, Inst. of Struct. Eng., Neubiberg, Germany, thomas.braml@unibw.de

Abstract:

The results of and the validity in reliability assessment of existing bridges essentially depend on the information available about the considered system. Information about the actual condition as well as structural and material characteristics can be observed on-site to refine the computation models used in assessment. Non-destructive testing (NDT) methods for concrete structures are capable of reconstructing missing, questioned, or inconsistent as-built plans. This contribution summarizes recent developments within the scope of the national pre-standardization project “ZfPStatik”, which aims to prepare a guideline about NDT-supported structural analyses. The focus is on the purposeful and explicit utilization of geometrical tendon and reinforcement bar positions (measured on-site using the ultrasound echo and ground penetrating radar (GPR) techniques) in probabilistic reliability analyses — shown by means of real case studies. The well-established first order reliability method is applied to different concrete bridges, which are typical for the German road bridge stock, to demonstrate the utility of incorporating quality-evaluated NDT-results in terms of changes in structural reliability.

Keywords: Non-destructive testing, prestressed concrete, FORM, data-informed reliability analysis

1 Introduction

The reliability analysis of existing structures employing measured data is particularly useful when required information is not available or incomplete, when justified doubts about the condition of available information have arisen, or when the available information is outdated. The non-destructive impulse echo methods, i.e., ultrasonics and ground penetrating radar, are capable to detect and measure, for example, component thicknesses and the position of tendons and steel rebars (see Figure 1). The significance of precise knowledge about these internal and external dimensions of structures became evident, e.g., in an analysis of 723 damage events that occurred primarily in European countries, some of which had considerable consequences [1]. In this study, 109 (15 %) of these damages were attributed to wrong dimensions or to the incorrect placement of the reinforcement. An example of deviations determined with the aforementioned volume methods can be found in [2]. If no verified construction documents are available in the course of a structural reassessment, the as-built condition must be surveyed and compared with any existing plans [3]. A regional investigation of 157 bridges, which are public easements of German municipalities, e.g. revealed, that the as-built drawings of 42 bridges are missing [4]. According to [5], it cannot be taken for granted that the as-built documents are complete and legible. An example in which the available documents were insufficient for the recalculation of a federal highway bridge can be found in [6].

Against this background, the present contribution addresses the clarification of the inner structure of concrete bridges (position of tendons and reinforcement bars) with the aim to explicitly incorporate quality-assured, measured information into the reliability assessment of existing structures. The methodology is summarized in sect. 2. The case studies presented in section 3 are part of the national, German pre-standardization project *ZfPStatik*, which aims at the subsequent structure-specific and measurement data-based modification of partial safety factors [7].

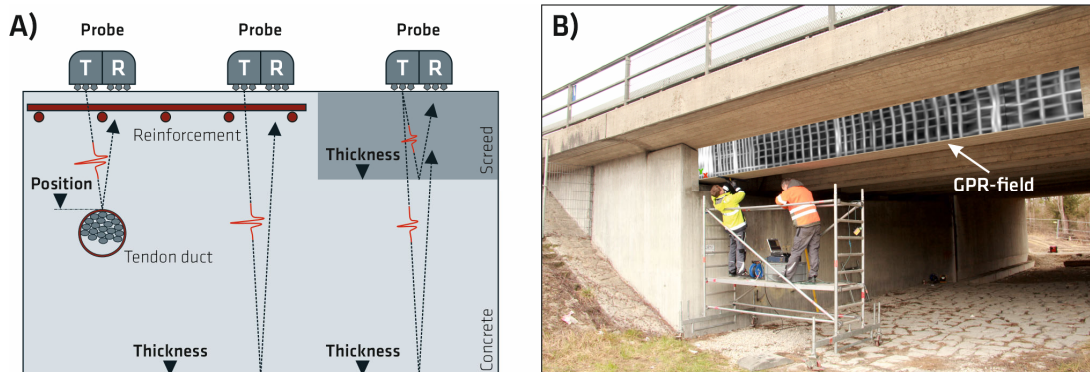


Figure 1: A) Principle of impulse echo methods [8]; B) One of the investigated bridges with GPR results indicating reinforcement bars inside a prestressed concrete bridge girder [9]

2 Methodology

The procedure for the reliability assessment of existing road bridges in Germany is specified in the recalculation guideline [3,10]. Once the recalculation premises (e.g., the target load level) have been defined and the available documents on the structure have been reviewed, structural analyses are performed, the evaluated and verified results of which are provided to the owner of the structure who determines the further actions to be taken. The visual inspection or any specific structural testing is not mandatory when evaluating structural reliability. The respective observations can, however, increase the level of approximation of the computation models. One available information source are non-destructive testing methods. NDT-supported reliability assessment can be guided by the following enhanced reassessment procedure:

1. Reliability assessment without measured data
Aim: Definition of quantities to be measured and specification of needed testing accuracies.
2. Non-destructive bridge inspections
Aim: Quality-evaluated NDT- and measurement results characterizing properties of the investigated structure.
3. Reliability assessment using measured data
Aim: Refined reassessment results based on the quality-evaluated on-site testing results.

The three case studies excerpted in section 3 each address one of these steps, which are summarized below. Further details about the methodology can be found in [11].

2.1 Reliability assessment without measured data

The starting point for any data-informed assessment should be the purposeful definition of structural, environmental, and material characteristics, which have been found to be *measurable* and *relevant*, i.e., they have a non-negligible influence on the calculation results (such as the probability of failure). In the presented concept, the pre-investigations carried out for the demand-actuated definition of the on-site testing tasks include:

- a) semi-probabilistic analyses acc. to the German recalculation guideline,
- b) probabilistic analyses including sensitivity analyses and parametric studies, and
- c) expert judgements.

The recalculation guideline [3,10] distinguishes between four evaluation stages. Initially, an existing bridge is to be assessed according to the current design standards (*Eurocodes, DIN-Fachberichte*). If the results are unsatisfactory, deviating specifications, e.g., reduced safety factors, can be included in the second stage analysis. The third and fourth stages allow, in exceptional cases, the consideration of measurement results and the application of scientific methods such as probabilistic analyses.

The weak points of the structure identified during the recalculation, in combination with the experience of the engineers involved, are used to define the testing tasks. Probabilistic sensitivity analyses and parameter studies further allow for the numerical specification of necessary and/or sufficient inspection qualities.

2.2 Non-destructive bridge inspections

The pre-investigations are followed by the design of on-site inspections, i.e., the development of measurement strategies to solve the previously defined testing tasks considering the specified requirements on the inspection result accuracies. The resulting measurement procedures form the basis for on-site testing and contain, in the field of NDT, i. a., information about the object and material to be tested, the objective, time, area and scope of the test, required qualifications and responsibilities of the personnel involved, the measuring equipment, and the entire inspection process (functionality test, calibration, data recording, documentation, data processing and evaluation, etc.) [12]. As the incorporation of NDT results in safety-relevant calculations require sound knowledge about the quality, i.e., precision and trueness of the information measured, an essential part of data analysis is the calculation of measurement uncertainties. These also serve to ensure the comparability of measurement results and can be drawn on the Guide to the Expression of Uncertainty in Measurement framework (GUM) [13–15], which has been applied to non-destructive testing in civil engineering in [16]. A measurement result consists at least of the best estimate of the measurand (measured value \hat{y}), the associated standard measurement uncertainty $u(\hat{y})$, and the distribution type of the measurand Y .

2.3 Reliability assessment using measured data

A measurement result can then be utilized to stochastically model the considered basic variable on the basis of the NDT on-site inspections. Principle modelling issues like the choice of the distribution family, the tail-sensitivity-problem, competing models, statistical uncertainties and correlation may have to be appreciated. Prior knowledge can be considered via the Bayes' theorem, which is, however, delimited in this paper, since the geometrical quantities are considered time-invariant and since the data gathered at the case study structures can comprehensively describe the characteristics of interest. This is not necessarily the case. The NDT-based basic variable can then be

- a) explicitly incorporated into NDT-supported probabilistic reassessment (as random variables) [11], or
- b) used to derive characteristic values and modify partial safety factors for the semi-probabilistic reassessment, e.g., based on the design value method or the adjusted partial factor method [17].

3 Case studies

This section presents excerpts from three of the case studies investigated within the scope of the pre-standardization project *ZfPStatik*. Section 3.1 emphasizes the probabilistic pre-investigations comprising of sensitivity analyses and parametric studies, section 3.2 the non-destructive testing on-site including the measurement result computation and sect. 3.3 exemplary changes in reliability after incorporating NDT results. An overview of the further bridges considered can be found in [18].

3.1 Four-span prestressed concrete bridge with T-beam cross-section

Table 1 gives an overview of the construction details, the analysed limit states, the identified structural weaknesses, and the performed on-site inspections. Detailed information about the probabilistic decompression proof can be found in [11].

Table 1: Bridge profile I, photos taken by *BAM*

Bridge profile				
Existing bridge carrying a four-lane federal highway in Schleswig-Holstein, Germany				
Cross-section:	Slab- and-beam with two haunched main girders			
System:	Longitudinally and transversely prestressed, four span continuous beam			
Dimensions / m	Total length	Width	Beam height	Slab height
	95,80	> 23	1,2...1,6	< 0,50
Year of construction:	1980			
Investigated limit states acc. to German recalculation guideline (stage 2*) [3,10]:	ULS:			
	1. <i>Proof of the stirrup reinforcement (torsion, shear)</i>			
* All verifications not listed could already be performed successfully acc. to stage 1.	SLS:			
	2. <i>Decompression in transversal direction</i>			
	Fatigue:			
	3. <i>..of the shear reinforcement</i>			
	Target load level: LM 1			
Identified weaknesses:	<ol style="list-style-type: none"> Based on a girder grillage model, the decompression proof, the fatigue proof of the shear reinforcement, and the torsion proof of the stirrups could not be successfully performed. The bridge could be successfully assessed using a FE shell model; however, the plans contained inconsistent information about the transverse tendon curves. 			
Performed inspections:	- Vertical position of the transverse tendon ducts with ultrasound-echo and ground penetrating radar in decisive cross-sections			



The First Order Reliability Method (FORM) acc. to [19–21] has been used to compute sensitivity coefficients α_i , which quantify the sensitivity of the reliability index β (or the operational probability of failure P_f respectively) against small changes in the mean of the respective basis variable, and elasticities $e_{\tau,i}$ as values indicating the change of β when varying a distribution parameter τ of a basis variable by 1 %. Additional parametric studies serve to estimate the influence of larger changes in a distribution parameter. The limit state function for the decompression proof acc. to the Eurocodes is

$$\begin{aligned}
 g(\sigma_c) &= 0 - \left(\frac{N}{A} + \frac{M}{W} \right) = 0 - \left(\frac{N}{A} + \frac{M}{I_y} \cdot z_z \right) && \text{Equation (1)} \\
 &= 0 - \frac{\theta_{E,N} (N_G + N_{Q,TS} + N_{Q,UDL} + N_P + N_{K+S} + N_{SE} + N_T)}{h \cdot b} \\
 &\quad - \frac{\theta_{E,M} (M_G + M_{Q,TS} + M_{Q,UDL} + N_P \cdot z_p + M_{K+S} + M_{SE} + M_T)}{h^3 b / 12} \cdot \frac{h}{2} \quad \text{with } z_p = -\frac{h}{2} + d_{sp,y} + \epsilon,
 \end{aligned}$$

where N represents the sum of the normal forces and M of the bending moments derived from finite element calculations, A the cross-sectional area, and W the section modulus. The vertical position of the tendon ducts is one random variable needed to define the lever arm z_p between the cross-sectional center and the tendon axis, where $d_{sp,y}$ is the distance between slab undersurface and bottom of the tendon duct and ϵ the strand eccentricity. Figure 2c shows the effects of the uncertainty about the vertical position of the transverse tendons in one decisive cross-section on the stresses. One of the two alternative (and competing) tendon positions extracted from the information available prior to any on-site testing (plans, static calculations, structure record, etc.) was modeled stochastically to be able to quantify the significance of the tendon position probabilistically. Both the models and the descriptions of all basis variables can be found in [11].

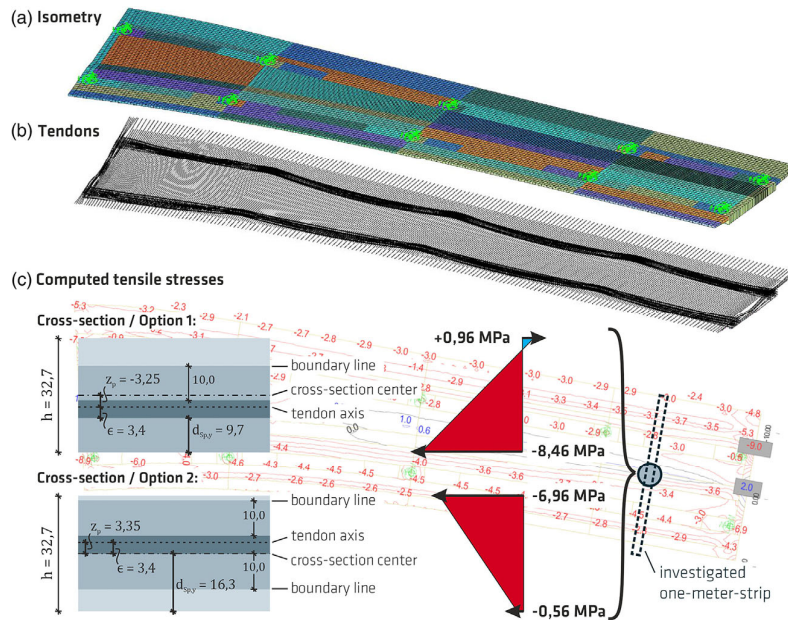


Figure 2: a) isometric FE shell model of the bridge; b) model of the tendons; c) tensile stresses / MPa considering both competing plan indications about the transverse tendon curve for the same cross-section; extracted from [11]

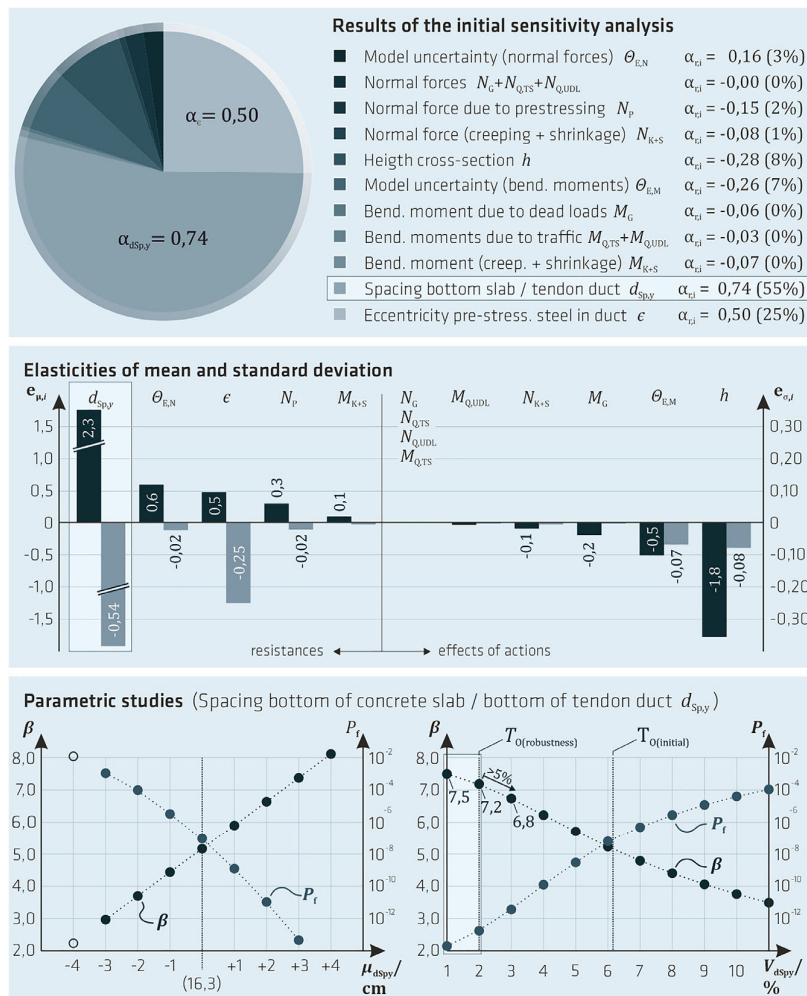


Figure 3: Sensitivity coefficients as well as elasticities of the mean and of the standard deviation of the respective basis variables as well as the reliability against changes in the mean and standard deviation of the spacing between slab undersurface and bottom of the transverse tendon ducts $d_{sp,y}$; extracted from [11]

The results of the pre-investigations are summarized in Figure 3 and reveal, regarding the tendon position $d_{sp,y}$, that:


- a squared sensitivity factor of $\alpha^2 = 55\%$ can be attributed to the vertical position of the transverse tendon ducts, which means that the basis variable $d_{sp,y}$ affects the computation results significantly and is therewith relevant,
- even a small deviation between the assumed and actual position (bias of the model) significantly influences reliability, which indicates an unrobust information basis prior to the on-site testing (see elasticities of the mean and $\beta = f(\mu_d)$),
- the reduction of the initially assumed scattering behaviour, which is based on the JCSS probabilistic model code [22], will be useful especially in the case of doubts about the condition (trueness, precision) of available information.

In order to decide justifiably which of both competing models describe the actual as-built position of the tendons and to reduce the uncertainty arising from the inconsistency of the information provided in the available documents, the curves of the transverse tendons especially in the areas, where the FE computations yield concrete edge tensile stresses, have been measured non-destructively through the application of the ultrasound and ground penetrating radar techniques on the slab undersurface. This serves to update the FE model and to derive the vertical tendon positions $d_{sp,y}$ over the transverse bridge direction y . The described study was published in [11] and is currently being further developed for all different proofs within the scope of the reassessment. The following case study is used to demonstrate, how such geometrical NDT results can be processed, visualized, and transferred into NDT-based stochastic models.

3.2 Single-span prestressed concrete bridge with partly prefabricated T-beam cross-section

Table 2 gives an overview of the construction details, the analysed limit states, the identified structural weaknesses, and the performed on-site inspections.

Table 2: Bridge profile II, photos taken by *BUNG Ingenieure AG*

Bridge profile				
Former existing bridge carrying a motorway with (in total) four lanes in Bavaria, Germany				
Cross-section:	Slab-and-beam with six prefabricated main girders			
System:	Longitudinally prestressed, single-span beam			
Dimensions / m	Total length	Width	Beam height	Slab height
	18,50	15,00	0,71	0,25
Year of construction:	1978			
Investigated limit states acc. to German recalculation guideline (stage 1 & 2) [3,10]:	ULS: 1. <i>Robustness reinforcement</i> 2. <i>Bending and axial force</i> 3. <i>Shear and torsion</i> 4. <i>Fatigue (concrete + steel)</i> 5. <i>Thrust beam web / flange</i> SLS: 6. <i>Decompression</i> 7. <i>Concrete, reinforcement + prestressing steel stresses</i> 8. <i>Crack width limitation</i> Target load level: LM 1			
				
Identified weaknesses:	1. Insufficient longitudinal reinforcement in the t-beam to withstand combined torsion and bending effects of actions and fatigue 2. Insufficient transversal reinforcement in the slab to withstand bending moments in transversal direction 3. Insufficient shear reinforcement in the beams (at least acc. to stage 1) 4. For a sufficient proof of decompression ($\sigma_c < 0$), the tensile strength of the concrete needed to be entered into the calculation ($0 < \sigma_c < f_{ctk,0.05}$)			
Performed inspections:	<ul style="list-style-type: none"> - Core drilling for determining the concrete quality and strength - Localization of the stirrups, especially in the transition area between densely and less reinforced zones - Localization of the tendons to validate the highly utilized decompression proof and to avoid collisions during the core drilling - Localization of the reinforcement in the slab (transversal and longitudinal) 			

The structure was built in 1978 and carries a motorway. The deck is composed of six precast T-girders connected by a 25 cm thick cast-in-place concrete layer. During the assessment, both ultimate limit state (ULS) and serviceability limit state (SLS) deficiencies were identified. The insufficient longitudinal reinforcement is mainly due to compatibility torsion and caused by the twisting of the beams due to transverse load distribution in the concrete slab. The transverse reinforcement in the slab is further insufficient to withstand the acting bending moments in transverse directions. The statically critical positions are shown in Figure 4.

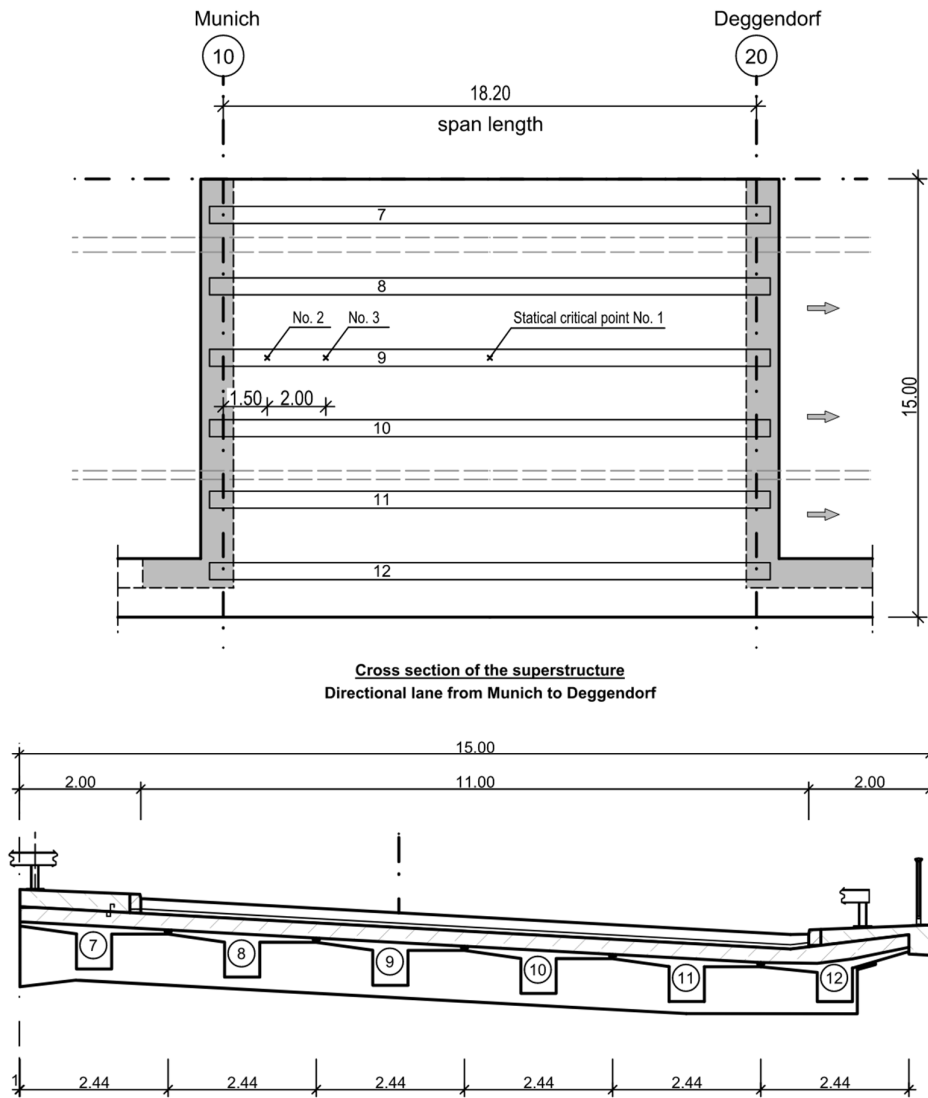


Figure 4: Top-view and cross section of the single-span PC bridge with partly prefabricated T-beams

The utilization rate of the existing stirrup reinforcement under shear forces in assessment stage 1 is comparably high, with local exceedances of up to 8%. However, these high utilization rates mostly occur at the transition areas between densely and less reinforced zones, which could be solved if the areas of more stirrup reinforcement were slightly extended. To address this, the stirrup reinforcement is being located using NDT as such slight exceedances and their handling often lead to discussions in practice. There are three tendons in each precast element, and their exact positions in horizontal and vertical directions were modeled in the finite element model according to the tendon layout plan, which gives defined support points. The slope and position of the tendons are also important, as they influence the shear resistance. The layout and position of the tendons significantly affect the bending moment distribution and impact the decompression. In the assessment stage 1, the verification of decompression was achieved by considering the tensile strength of concrete. Since the decompression proof is highly utilized here, the exact positions of the tendons have been measured simultaneously with the stirrup spacing and positions of stirrup density changes in longitudinal bridge direction. Furthermore, the concrete strength is relevant for approximating the tensile strength of concrete.

In localization of inner structural components (rebars, tendons, etc.) based on the non-destructive volume methods GPR and ultrasonic pulse echo, time domain signals are recorded as raw data on-site. A number of these time domain signals (see Figure 5a), which have been collected at a number of equidistant measuring points, can be color-coded and stacked in order to derive cross-sections cutting the investigated component perpendicularly to the measuring line (see Figure 5b). Reconstruction algorithms, e.g., the Synthetic Aperture Focusing Technique (SAFT), can be used to focus a set of signals reflected by an object to the origin of the reflection (Figure 5c). In order to localize the detected reflectors in a spatially resolved volume, it is required to know the individual propagation velocity of the pulse within the measuring object, as $d = vt/2$ (d – reflector depth; v – propagation velocity; t – time of flight) in echo arrangement of the antennas or probes. Provided that the quantities are considered as random variables, inserting the best estimates of the velocity \hat{v} and time of flight \hat{t} into this equation yields the best estimate of the reflector depth \hat{d} . When additionally applying the Gaussian error propagation law to the aforementioned equation, the resulting value can be seen as a measure to describe the uncertainty related to the best estimate \hat{d} . The definition of the quantity to be measured $Y = d$, the identification and stochastic modeling of the input quantities $X_1 = v$; $X_2 = t$ and the formulation of their mathematical relationship $Y = f(X_i)$ are the major challenges in calculating measurement uncertainties. Even if this modeling of a measurement is more complex in most cases, the application of the broadly applicable and internationally accepted rules [13] provided in the Guide to the Expression of Uncertainty in Measurement (GUM) to a model leads to clearly interpretable and comparable measurement results – at least consisting of the measured quantity value \hat{y} , the standard measurement uncertainty $u(\hat{y})$ describing the measurement uncertainty as a standard deviation and the distribution type of the measurand Y . In this way, the raw data can be transferred into quantitative, quality-assessed characteristics of the structure. Approaches to the development of measurement models for ultrasonic and ground penetrating radar inspections at concrete bridges can be found in [23,24].

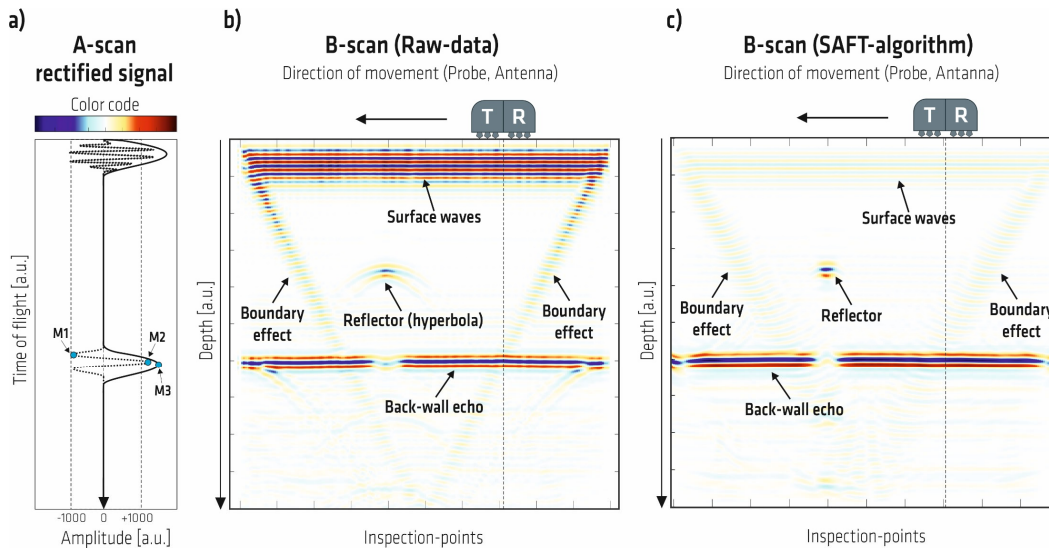
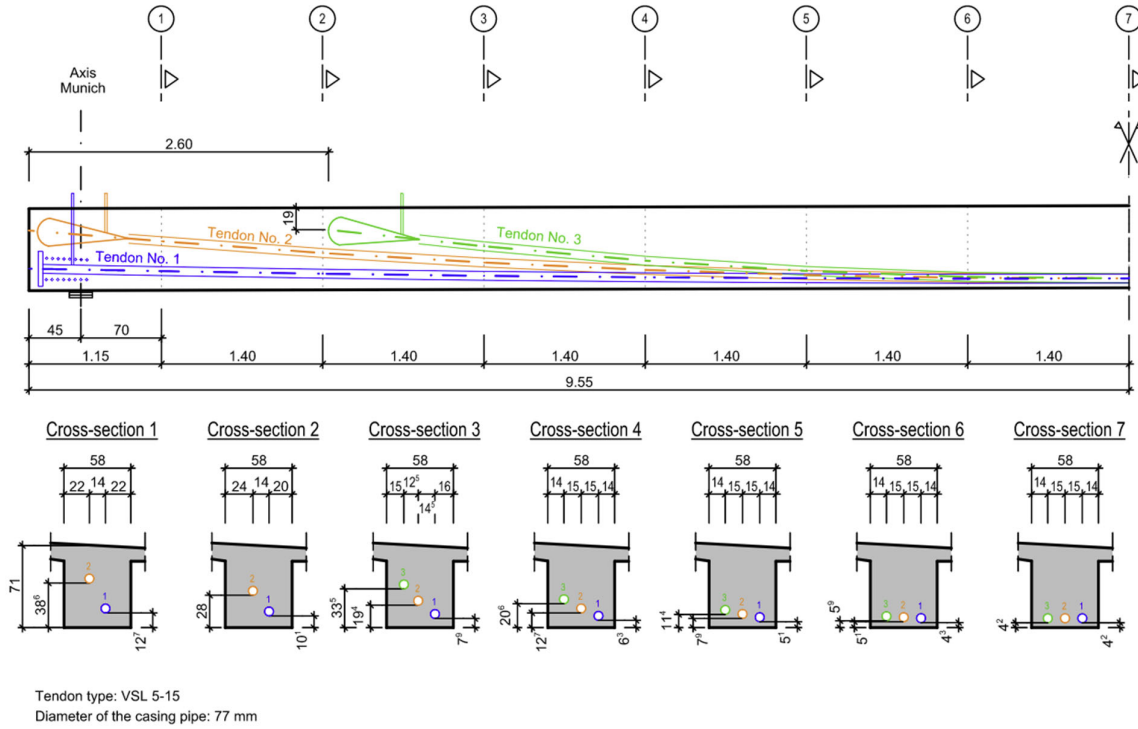


Figure 5: Imaging of ultrasound data; a) single time domain signal; b) color-coded and stacked time domain signals yield the cross-section; c) reconstructed cross-section with focused reflector indication; extracted from [25]

The GUM procedure has been also applied to the GPR data collected at the present motorway bridge, amongst others, to determine the curves of the longitudinal tendons within the main girders. The indicated values should be understood as best estimates of the vertical tendon position in the respective axis. The associated standard uncertainties $u(\hat{y})$ take on values of approx. one centimeter, which means, that the interval $\hat{y} \pm 1 \text{ cm}$ contains the (unknown and theoretical) “true” value of the tendon duct position with a probability of ca. 65 %, as Y follows a normal distribution $Y \sim N(\hat{y}, u(\hat{y}))$. The NDT-based basic variable can then be modelled based on the distribution type and parameters defined for the measurand.

Figure 6 shows the various positions of the tendons, which follow a polygonal path. According to the plan documents, support points are given at intervals of 140 cm, where the distance between the casing pipe and the bottom of the cross-section is specified. This plan data applies to all twelve girders equally. The measurement results are provided for girders 9, 10, and 12, and there is generally a good agreement in the number and path of the tendons, as seen in Figure 7. The deviations between planned and measured values range from 0 to 4 cm, with a tendency towards lower-lying tendons. The effects of these deviations will be analyzed and evaluated in the further progress of the project. In this context, it will also be investigated whether the reduction of the statically effective lever arm Δd_s by two centimeters prescribed in the recalculation guideline, if the partial safety factor γ_s is to be reduced to 1.05, can be dispensed with, i.e. whether this additive safety element can be alternatively covered by reducing the uncertainties through on-site NDT without restricting the normative reliability level.

Longitudinal section (girder 1 to 12)



	Cross-section 1			Cross-section 2			Cross-section 3			Cross-section 4			Cross-section 5			Cross-section 6			Cross-section 7									
	nominal value from documents	Measured value girder No.			nominal value from documents	Measured value girder No.			nominal value from documents	Measured value girder No.			nominal value from documents	Measured value girder No.			nominal value from documents	Measured value girder No.			nominal value from documents	Measured value girder No.						
		9	10	12		9	10	12		9	10	12		9	10	12		9	10	12		9	10	12	9	10	12	
Tendon No. 3	-	-	-	-	-	-	-	33.5	33.95 (+0.45)	32.15 (-1.35)	32.45 (-1.05)	20.6	20.65 (+0.05)	19.65 (-0.95)	20.55 (-0.05)	11.4	11.65 (+0.25)	11.25 (-0.15)	11.55 (+0.15)	5.9	2.65 (-3.25)	/	3.05 (-2.85)	4.2	2.15 (-2.05)	/	2.65 (-1.55)	
Tendon No. 2	38.6	37.25 (-1.35)	36.95 (-1.65)	35.95 (-2.65)	28.0	28.55 (+0.55)	26.15 (-1.85)	26.65 (-1.35)	19.4	17.15 (-2.25)	17.95 (-1.45)	17.15 (-2.25)	12.7	10.65 (-2.05)	10.45 (-2.25)	10.65 (-2.05)	7.9	7.00 (-0.90)	/	4.15 (-3.75)	5.1	2.65 (-2.45)	/	3.05 (-2.05)	4.2	2.15 (-2.05)	/	2.65 (-1.55)
Tendon No. 1	12.7	12.35 (-0.35)	11.85 (-0.85)	14.15 (+1.45)	10.1	10.05 (-0.05)	8.75 (-1.35)	9.65 (-0.45)	7.9	6.65 (-1.25)	5.95 (-1.95)	6.05 (-1.85)	6.3	2.45 (-3.85)	2.55 (-3.75)	3.35 (-2.95)	5.1	2.65 (-2.45)	2.55 (-2.55)	3.35 (-1.75)	4.3	2.65 (-1.65)	/	3.05 (-1.25)	4.2	2.15 (-2.05)	/	2.65 (-1.55)

The values are measured in centimetres from the bottom of the girder to the bottom of the casing pipe.

Figure 6: Position of the tendons in the prestressed concrete girders

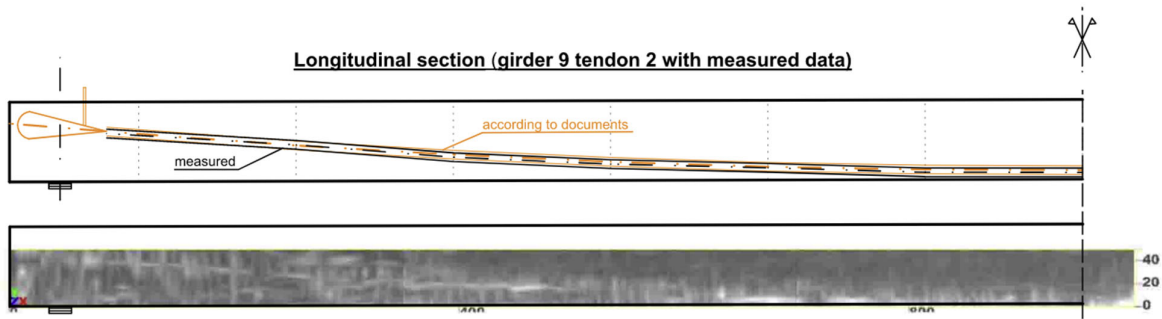




Figure 7: Comparison of the tendon position according to plan and NDT (top) and imaging of the center tendon (no. 2) mounted in a depth related to the measuring area, which approximately corresponds to the maximum penetration depth of the electromagnetic waves used for GPR testing in this case (bottom)

3.3 Three-span prestressed concrete bridge with single-cell hollow box cross-section

The focus of this section is on the demonstration of conceivable changes in structural reliability after incorporating geometrical NDT results into the reassessment. Table 3 gives an overview of the construction details, the analysed limit states, the identified structural weaknesses, and the performed on-site inspections. Further information about the probabilistic bending and shear (tension strut) proof including all stochastic models can already be found in [26].

Table 3: Bridge profile III, photos taken by *HFR Ingenieure GmbH* and *BAM*

Bridge profile				
Former existing bridge carrying a two-lane federal highway in Bavaria, Germany				
Cross-section:	Single-cell hollow box with variable height			
System:	Longitudinally and transversely prestressed, three span continuous beam			
Dimensions / m	Total length	Width	Construction height	
	133	12	1,20 ... 1,45	
Year of construction:	1965			
Investigated limit states acc. to German recalculation guideline (stage 1 & 2) [3,10]:	ULS in longitudinal direction: 1. <i>Robustness reinforcement</i> 2. <i>Bending and axial force</i> 3. <i>Shear and torsion</i> SLS in longitudinal direction: 4. <i>Decompression</i> 5. <i>Concrete, reinforcement + prestressing steel stresses</i> 6. <i>Crack width limitation</i> Target load level: LM 1			
Identified weaknesses:	1. insufficient amounts of reinforcement to avoid failure without prior notice only in the areas around the moment zero points (uncritical) 2. serious deficits in the tension strut and deficits in the compression strut proof 3. insufficient amount of reinforcement to connect the slabs to the webs 4. minor deficits in decompression proof and torsion analysis			
Performed inspections:	- structural clarification: detection and localization of the longitudinal tendons in center span and the shear reinforcement (pier area) using ultrasound and GPR, - half-cell potential (corrosion activity), concrete cover, air permeability [27], - concrete strength using drill cores, and further monitoring activities including proof load tests.			

The limit state function that has been used to assess the bridge regarding the ultimate limit state (ULS) bending considering the compressive reinforcement is given in [28]:

$$g(M_R) = U_{R,M} \cdot \left(A_{sp} \cdot f_p \cdot (h - d_{sp} - d_2) + a_R \cdot b \cdot \xi \cdot (h - d_{sp}) \cdot 0,85 \cdot f_c \cdot (d_2 - k_a \cdot \xi \cdot (h - d_{sp})) \right) - U_E \cdot (M_G + M_Q + M_{VP}) \quad \text{Equation (2)}$$

The tension strut proof, as a part of the shear assessment, is based on the following function published in [28]:

$$g(V_{R,s}) = U_{R,s} \cdot \left(\frac{A_{sw}}{s_w} \cdot f_y \cdot (0,9 \cdot (h_s - d_1)) \cdot (\cot \theta + \cot \alpha) \cdot \sin \alpha \right) - U_E \cdot (V_G + V_Q + V_P) \quad \text{Equation (3)}$$

The relevant basic variables included in equations (2) and (3) are described in Figure 8. A list of all stochastic models can be found in [26]. The considered (and non-destructively measured) stochastic models of the respective geometrical basic variables are compared in Table 4. It can be derived a) from the comparably small changes in the means, that the plans and further information available prior to any measurements appropriately reflect the as-built condition in this specific case, and b) that the uncertainty could be significantly reduced through the on-site inspections.

The initial models listed in Table 4 were substituted by the respective NDT-based basic variables and the initial reliability analyses then repeated using the FORM. The effects of including the NDT results on the computed values are summarized in Figure 8. The values of the reliability index increase by + 13 % in ULS shear and + 4 % in ULS bending. The alpha-values of the NDT-based basic variables tend to zero as the measurement uncertainty has been found to be comparably small and the respective quantities thus stochastically insignificant. The elasticities of the means indicate that a larger bias

between the as-planned and as-built shear stirrup spacing $\Delta\mu_{sw}$ would affect structural reliability significantly. Although a bias of the vertical tendon position d_{sp} has a less impact on reliability, it can however be derived, e.g., from $e_{\mu,h} = 1,55$ that the inner lever arm z remains to significantly influence structural reliability in ULS bending.

Table 4: Models of investigated basic variables based on the information prior to (initial) and after the on-site testing

Basic variable (initial)	Distribution type and parameters			Basic variable (NDT-based)	Distribution type and parameters		
	Type	Mean	CoV		Type	Mean	Cov
Tendon position d_{sp}	Normal	0,247 m	12 % [22]	Tendon pos. d''_{sp}	N	0,223 m	0,6 %
Spacing stirrups s_w	Normal	0,15 m	6,7 % [22]	Spacing s''_w	N	0,148 m	0,1 %
Prestr. ($M_{cp,ind}$) M_{VP}	Normal	13,279 MNm	5,0 %	Prestr. M_{VP}''	N	13,763 MNm	5,0 %

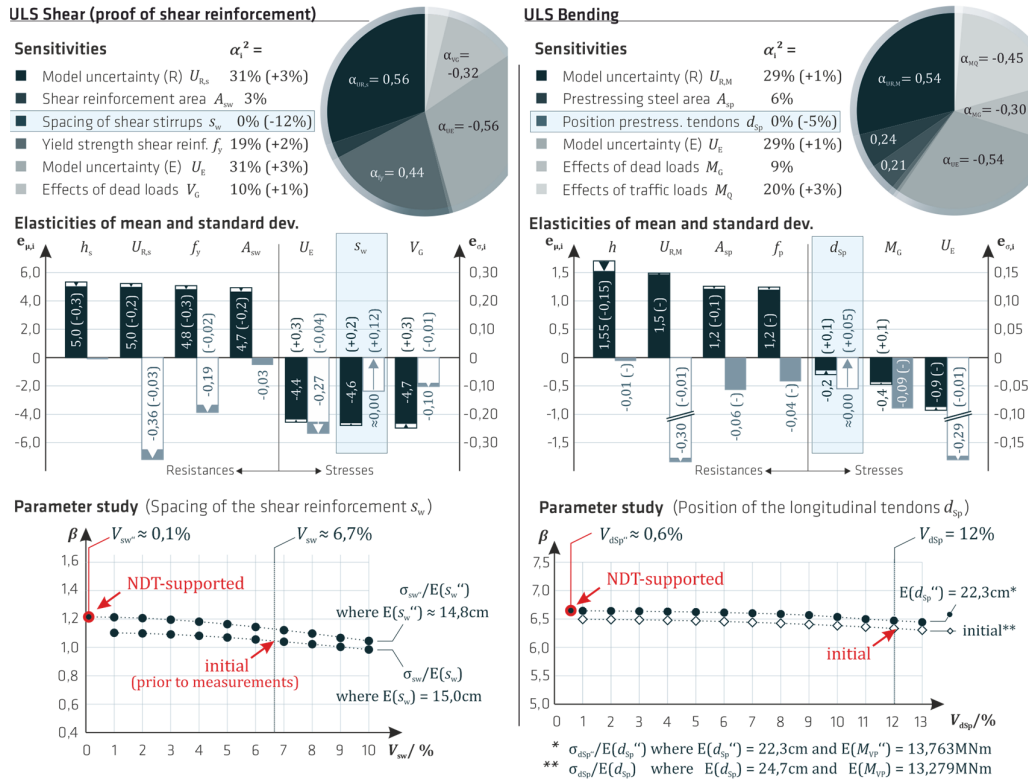


Figure 8: Results of the reliability reassessments in ULS shear (left) and ULS bending (right); the changes in computed sensitivity coefficients and elasticities after incorporating the geometrical NDT results are indicated in brackets; changes in reliability index are plotted at the bottom; extracted from [26]

4 Conclusion

This contribution summarizes the main steps in probabilistic NDT-supported reliability assessment of existing bridges by means of excerpts of three different case studies that are currently investigated within the scope of the German pre-standardization project *ZfPStatik*. First, the ways to purposefully define quantities to be measured on-site, second, the on-site testing and data analysis, and third, the impact of including NDT results in the assessment on calculated reliability have been shown in three assessment scenarios. The aim of the overall project is the integration of most modern inspection methods into the assessment process of existing structures by supplementing the current rules with a practicable and code-compliant procedure for NDT data-based, structure-specific modifications of partial safety factors. This will facilitate more realistic structural assessments, optimized maintenance strategies, higher infrastructure availability and, in general, the targeted allocation (and thus conservation) of resources. In the next step, the already completed semi-probabilistic recalculations of six prestressed concrete bridges will be enhanced by further probabilistic reliability (and sensitivity) analyses. Most of the on-site inspections have already been carried out – with a focus on geometrical quantities as well as the compressive strength of the concrete. Currently, the NDT results are being successively integrated into the reassessments in order to investigate, to what extent the values of the partial safety factors can be modified depending on the type and extent of non-destructive on-site inspections. The project will be completed in summer 2024.

Acknowledgement

The authors gratefully acknowledge the valuable activities of all project partners, esp. M. Keuser, A. Soukup and J. Wöstmann, as well as the financial support of the German Federal Ministry for Economic Affairs and Climate Action under grant number 03TN0042.

5 References

- [1] Matousek M., Schneider J.: Untersuchungen zur Struktur des Sicherheitsproblems bei Bauwerken. Bericht / Institut für Baustatik und Konstruktion ETH Zürich, 59 1976.
- [2] Taffe A. et al.: Bauwerkscanner zur automatisierten und kombinierten Anwendung zerstörungsfreier Prüfverfahren im Bauwesen. *Beton- und Stahlbetonbau*, 106 (4) 2011, p. 267–276. doi:10.1002/best.201100004.
- [3] Bundesministerium für Verkehr, Bau und Stadtentwicklung: Richtlinie zur Nachrechnung von Straßenbrücken im Bestand (Nachrechnungsrichtlinie). 05/2011.
- [4] Rechnungshof Rheinland-Pfalz: Bericht nach § 111 Abs. 1 LHO über die Erhaltung und den Zustand von Brücken in kommunaler Baulast: Az.: 2-P-0057-39-1/2011. Speyer, 10.10.2013.
- [5] Marzahn G.: Die Tragfähigkeitsreserven vieler älterer Brücken sind weitgehend aufgebraucht: Zur Weiterentwicklung der Nachrechnungsrichtlinie für die Entscheidung über Verstärkung oder Ersatz. *Der Prüfenieur*, (42) 2013, p. 20–29.
- [6] Maack S., Diersch N.: Einsatz von zerstörungsfreien Prüfverfahren (ZfP-Verfahren) zur Rekonstruktion von Bestandsplänen als Grundlage für die Nachrechnung: Schlussbericht für das Forschungsprojekt FE 29.0333/2013/BAST. Berlin, 2015.
- [7] BAM: Bridge safety - closures and expensive renewals could often be avoided through state-of-the-art testing methods: <https://www.bam.de/Content/EN/Press-Releases/2022/Infrastructure/2022-12-01-bridge-safety-testing-methods.html> (retrieved 2023-06-23). Press release. Berlin, 2022.
- [8] Maack S. et al.: Die Ultraschall - Echomethode – von der Messung zur bautechnischen Kenngröße. *Beton- und Stahlbetonbau*, 116 (3) 2021, p. 200–211. doi:10.1002/best.202000091.
- [9] Küttenbaum S. et al.: Ways to unlock the potential of non-destructive concrete testing for the reliability assessment of our built environment. In: 8th International Workshop on Reliability of NDT/NDE @ SPIE Smart Structures + Nondestructive Evaluation 2023 (Editors: D. Kanzler, N. G. Meyendorf). SPIE, 12.03.2023 - 17.03.2023, p. 1249107-1...11. doi: 10.1117/12.2658736.
- [10] Bundesministerium für Verkehr und digitale Infrastruktur: Richtlinie zur Nachrechnung von Straßenbrücken im Bestand (Nachrechnungsrichtlinie). 04/2015.
- [11] Küttenbaum S. et al.: Reliability assessment of existing structures using results of nondestructive testing. *Structural Concrete*, 22 (5) 2021, p. 2895–2915. doi:10.1002/suco.202100226.
- [12] Deutsche Gesellschaft für zerstörungsfreie Prüfung e.V.: Richtlinie B-LF 01: Leitfaden zur Erstellung von Prüfanweisungen für die Zerstörungsfreie Prüfung im Bauwesen (ZfPBau). Berlin, 04/2022.
- [13] Joint Committee for Guides in Metrology: JCGM 100:2008. Evaluation of measurement data — Guide to the expression of uncertainty in measurement. 2008.
- [14] Joint Committee for Guides in Metrology: JCGM 101:2008. Evaluation of measurement data — Supplement 1 to the “Guide to the expression of uncertainty in measurement” — Propagation of distributions using a Monte Carlo method. 2008.
- [15] Joint Committee for Guides in Metrology: JCGM 102:2011. Evaluation of measurement data – Supplement 2 to the “Guide to the expression of uncertainty in measurement” – Extension to any number of output quantities. 2011.
- [16] Taffe A.: Zur Validierung quantitativer zerstörungsfreier Prüfverfahren im Stahlbetonbau am Beispiel der Laufzeitmessung. 1st ed. Berlin, Wien u.a.: Beuth, 2008.
- [17] International Federation for Structural Concrete: Partial factor methods for existing concrete structures: Recommendation. Bulletin 80. Lausanne, Switzerland: Fédération internationale du béton, 2016.
- [18] Küttenbaum S. et al.: Guideline on NDT-supported reliability assessment of existing structures – Current developments in Germany. ce papers: EUROSTRUCT 2023 Conf. proc., BOKU Vienna, Sep. 2023, accepted.
- [19] Hasofer A. M., Lind N. C.: Exact and Invariant Second-Moment Code Format. *Journal of the Engineering Mechanics Division*, 1974 (100) 1974, p. 111–121.
- [20] Rackwitz R., Fiessler B.: Structural reliability under combined random load sequences. *Computers & Structures*, 9 (5) 1978, p. 489–494. doi:10.1016/0045-7949(78)90046-9.
- [21] Hohenbichler M., Rackwitz R.: Non-Normal Dependent Vectors in Structural Safety. *Journal of the Engineering Mechanics Division*, 107 (EM6) 1981, p. 1227–1238.
- [22] JCSS: Probabilistic Model Code: Part 1-3. Zurich: Joint Committee on Structural Safety, 2001/2002.
- [23] Küttenbaum S. et al.: On the treatment of measurement uncertainty in stochastic modeling of basic variables. *APP*, 36 2022, p. 109–118. doi:10.14311/APP.2022.36.0109.
- [24] Küttenbaum S. et al.: Approach to the development of a model to quantify the quality of tendon localization in concrete using ultrasound. *MATEC Web Conf.*, 364 2022, p. 3007. doi:10.1051/mateconf/202236403007.

- [25] Maack S. et al.: Practical procedure for the precise measurement of geometrical tendon positions in concrete with ultrasonic echo. MATEC Web Conf., 364 2022, p. 3008. doi:10.1051/mateconf/202236403008.
- [26] Küttenbaum S. et al.: Towards NDT-supported decisions on the reliability of existing bridges. In: ICOSAR 2021-2022, 13th International Conference on Structural Safety & Reliability (Editors: J. Li et al.). 2023, in print.
- [27] Maack S. et al.: Testing to Reassess – Corrosion Activity Assessment Based on NDT Using a Prestressed Concrete Bridge as Case-Study. In: Proceedings of the 1st Conference of the European Association on Quality Control of Bridges and Structures (Editors: C. Pellegrino et al.). Cham: Springer International Publishing, 2022, pp 678–686.
- [28] Braml T.: Zur Beurteilung der Zuverlässigkeit von Massivbrücken auf der Grundlage der Ergebnisse von Überprüfungen am Bauwerk. Zugl.: Neubiberg, Univ. der Bundeswehr München, Diss., 2010. Düsseldorf: VDI-Verlag, 2010.